Contemporary Mathematics
http: //ojs.wiserpub.com/index.php/CM/

Research Article

A Time-Delayed Model and Estimation in Parabolic-Trough Solar Collectors

Sharefa Asiri

Department of Mathematics, King Abdulaziz University, Jeddah, Saudi Arabia
E-mail: smaasiri@kau.edu.sa

Received: 15 September 2024; **Revised:** 20 November 2024; **Accepted:** 26 November 2024

Abstract: The dynamics of the parabolic-trough solar collectors are described by a differential equation model. Based on this model, different control strategies have been proposed to manage the heat production. However, the time delay between the solar irradiance (input) and the outlet temperature (output) has not yet been incorporated into the model. Considering this parameter will improve the model-based control techniques that strongly depend on the solar irradiance function. This paper develops a mathematical model for the parabolic-trough solar collectors in which the time delay is included. Since this parameter is unknown in practice, a method based on a cross-convolution approach is proposed to estimate it accurately. Moreover, the efficiency of the proposed method is improved by combining it with a filtering methodology. The proposed model's effectiveness and the estimation method's performance are demonstrated through numerical simulations.

***Keywords*:** distributed solar collectors, delay estimation, cross-convolution approach

MSC: 60G35, 76-10, 93-10, 93E10, 93C43

1. Introduction

The need to reduce CO_2 emissions from conventional electricity generation, such as fossil fuels, is driving the development and research in renewable energy sources [1]. Solar energy stands out as the most abundant renewable energy resource. This study focuses on Parabolic-Trough Collectors (PTC). One of the significant features of these solar plants is their ability to store energy, which can be utilized later, such as during nighttime [2]. PTC plants utilize concentrated sunlight to generate thermal energy through heat transport along collector tubes. Parabolic mirrors are employed to concentrate solar irradiance onto a central tube, where it is absorbed and carried by a heat carrier fluid to the collector outlet (refer to Figure 1). A differential equation model has been developed to provide a comprehensive depiction of the solar field regarding the fluid's internal energy variation [3–5]. Based on this model, extensive research has been conducted to design control strategies for managing and enhancing heat production. The control problem is to establish a law based on the fluid flow rate to maintain the outlet temperature around a specified desired reference [6]. Most of the model-based control techniques strongly depend on the solar irradiance, which is in the model a function of time [3–5, 7, 8]. However, the model does not consider the time delay between the solar irradiance (input) and the outlet

DOI: https://doi.org/10.37256/cm.5420245727

temperature (output). This delay is primarily due to the thermal inertia of the receiver tube and the heat transfer fluid. When the solar irradiance increases, it takes time for the receiver tube and the fluid to absorb and reach higher temperatures. Similarly, when solar irradiance decreases, it takes time for the temperature of the fluid to decrease. Therefore, considering this time delay in PTC's mathematical model is necessary to improve the control strategies, that consequently enhances the efficiency of heat production.

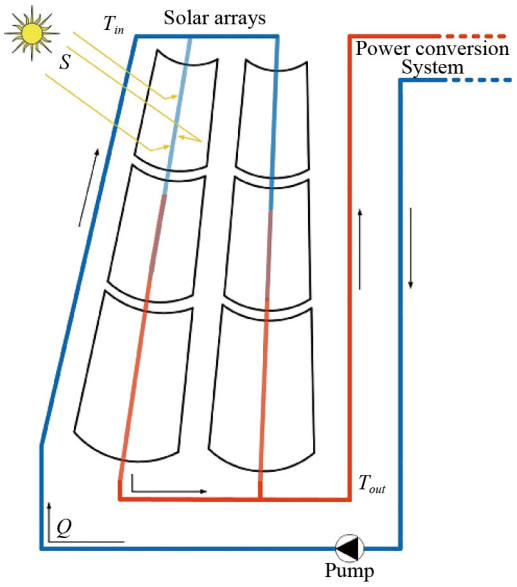

Figure 1. A diagram illustrating the hydraulic circuitry of a PTC

Nevertheless, the value of this time delay is uncertain or unknown due to changes in many factors, such as inlet temperature, fluid flow rate, ambient temperature, and mirror reflectivity. This motivates the estimation of the time delay using accessible measurements. Several approaches have been applied to identify time delays, such as a high-order sliding mode technique [9], recursive gradient method [10], variable structure observer [11], and variation of the least square method [12]. These approaches and most of the existing ones are either asymptotic or off-line. However, the time delay in PTC should be estimated during the plant operation. Asiri and Liu combined an algebraic approach with the Gauss-Newton method to estimate the time delay in a class of linear time-delay systems [13]. Although the method is fast and robust against noise, its performance is significantly affected by an initial guess.

In this work, the mathematical model is adapted to consider the time delay between the input and the output. In addition, the algebraic approach in [14, 15] is proposed for estimating this delay. By employing this method, the delay can be estimated through integral formulas without the need for iterative techniques or knowledge of initial conditions, leading to fast convergence. Furthermore, it is robust against noise in the outlet temperature due to the inclusion of integral terms [16]. It also operates in real-time, making it suitable for PTC. Moreover, the time delay can be estimated without knowing the optical efficiency of the mirrors, which is usually uncertain or unknown.

The rest of the paper is organized as follows. Some necessary formulas are recalled in Section 2. The adapted model and problem formulation are given in Section 3. Section 4 presents the time delay estimation approach. The results are investigated numerically in Section 5. Finally, the work is concluded in Section 6.

2. Preliminaries

This section revisits essential formulas that will play a crucial role in attaining the main results. Through the paper, the notation D^n and D^{-n} refer to the n^{th} derivative and the n^{th} integral, respectively.

Lemma 1 [17] Let $n,\ m \in \mathbb{N}$ with $n \geq m$ and $f \in C^m([0,\ t_f])$ [The space of functions that are m times continuously differentiable on $[0,\ t_f]$.], then

$$D^{-n}\{D^m f(t)\} = D_t^{m-n} f(t) - \Psi_{-n,\,m}\{f(t)\}, \tag{1}$$

where

$$\Psi_{-n,\,m}\{f(t)\} = \sum_{i=1}^{m} \frac{1}{\Gamma(1+n-i)}\ t^{n-i}\left[D^{m-i} f(t)\right]_{t=0}, \tag{2}$$

and $\Gamma(.)$ is the well known Gamma function [$\forall\ z \in \mathbb{C}$ with $R(z) > 0$, $\Gamma(z) := \int_0^\infty e^{-t} t^{z-1} dt$].

Lemma 1 can be seen as a repeated application to the fundamental theorem of calculus. The next theorem shows the act of the integral operator on convolution.

Theorem 1 [15, 18] Let $n \in \mathbb{N}$ and $f,\ g \in L^1([0,\ t_f])$ [$L^1([0,\ t_f]) = \{f :\ [0,\ t_f] \to \mathbb{R}|\ f$ is measurable on $[0,\ t_f]$ and $\int_0^{t_f} |f(t)|dt < \infty\}$], then

$$D^{-n}\{g(t) * f(t)\} = \int_0^t D^{-n} g(\tau)\ f(t-\tau)\ d\tau = D^{-n}\{g(t)\} * f(t), \tag{3}$$

where $*$ is the convolution operator [$f(t) * g(t) = \int_0^t f(t-\tau) g(\tau) d\tau$].

Remark 1 Lemma 1 and Theorem 1 have been stated in their references in the context of fractional calculus, more specifically, Riemann-Liouville type. Here, they were presented in terms of classical calculus on which this study is based. This adjustment is valid because the Riemann-Liouville integral generalizes the repeated antiderivative for positive integer orders.

3. Mathematical model and problem formulation

The overall description of the solar field in terms of the fluid internal energy variation is modeled by [3]

$$C_{loop}\frac{dT_{out}}{dt} = K_{opt} n_0 S\ I(t) - q P_{cp}(T_{out} - T_{in}) - H_l S(T_{mean} - T_a), \tag{4}$$

where C_{loop} is loop heat capacity in J/°C, T_{out} is outlet temperature in °C, K_{opt} is optical efficiency, n_0 is geometric efficiency, S is the total reflective surface in m^2, I is direct solar radiation in W/m^2, q is loop oil flow rate in m^3/s, P_{cp} is fixed factor based on loop geometrical and thermal properties in J/m^3 °C, T_{in} is inlet temperature in °C, H_l is thermal loss global coefficient in $W/(m^2$ °C), T_{mean} is the mean temperature between inlet and outlet temperature in °C, and T_a is ambient temperature in °C.

In this paper, the time delay between the solar irradiance (input) and the outlet temperature (output) is considered; hence, the following modified model is proposed

$$C_{loop}\frac{dT_{out}}{dt} = K_{opt}n_0S\ I(t-\delta) - qP_{cp}(T_{out}-T_{in}) - H_lS(T_{mean}-T_a), \tag{5}$$

where δ is a constant representing the delay.

The objective of this study is to solve the following Estimation Problem:

EP: Given the output $T_{out}(t)$, find the delay δ.

4. Delay estimation using cross-convolution approach

This subsection presents algebraic integral formulas for solving **EP** using a cross-convolution approach.

For convenience, Equation (5) will be written in the form:

$$a_1DT_{out} + a_2(T_{out}-T_{in}) + a_3(T_{mean}-T_a) = b\ I(t-\delta), \tag{6}$$

where $D := \frac{d}{dt}$, $a_1 = C_{loop}$, $a_2 = qP_{cp}$, $a_3 = H_lS$, and $b = K_{opt}n_0S$.

In the next theorem, the unknown delay δ is found using the cross-convolution approach (see the main steps of the approach in the flowchart in Figure 2).

Theorem 2 Let δ be unknown in (5), then it can be calculated as follows: $\forall t \in [0,\ t_f]$

$$\delta = \frac{\ln(\sqrt{\mu})}{\gamma}, \tag{7}$$

where

$$\mu = \frac{\int_0^t \left[Y(\theta) *\ e^{-\gamma\theta}\ I(\theta)\right]^2 d\theta}{\int_0^t \left[e^{-\gamma\theta}Y(\theta) *\ I(\theta)\right]^2 d\theta}, \tag{8}$$

such that $Y(t)$ represents the left hand side (L.H.S) of (6), and γ is a tuning parameter.

Proof. First, let's write Equation (6) in the following short form:

$$Y(t) = b\ I(t-\delta) \tag{9}$$

Step 1: Multiplying (9) by a continuous function $\alpha(t-\delta)$:

$$\alpha(t-\delta)\ Y(t) = b\ (\alpha I)(t-\delta), \tag{10}$$

Step 2: Convolving the L.H.S of (10) with the R.H.S of (9) and the R.H.S of (10) with the L.H.S of (9):

$$\alpha(t-\delta)Y(t) * b\ I(t-\delta) = Y(t) * b\ (\alpha I)(t-\delta), \tag{11}$$

which can be written as

$$\alpha(t-\delta)Y(t) * b\ I(t) = Y(t) * b\ (\alpha I)(t). \tag{12}$$

Notice that by this step, δ is neither in the input I nor in the output T_{out}.

Step 3: Let $\alpha(t) = e^{-\gamma t}$, then $\alpha(t-\delta) = e^{-\gamma t}\ e^{\gamma\delta}$. Hence,

$$e^{\gamma\delta}\left\{e^{-\gamma t}\ Y(t) * b\ I(t)\right\} = Y(t) * b\ e^{-\gamma t}\ I(t). \tag{13}$$

Therefore,

$$e^{\gamma\delta} = \frac{Y(t) *\ e^{-\gamma t}\ I(t)}{e^{-\gamma t}Y(t) *\ I(t)}. \tag{14}$$

Step 4: Taking the natural logarithmic function to both sides of (14), then squaring and integrating (to avoid singularities that might result from the zero crossing of the denominator) complete the proof. □

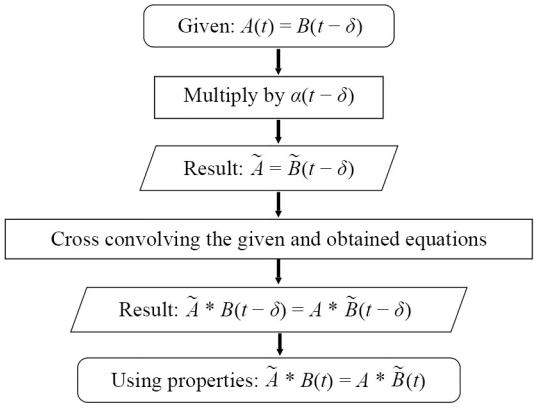

Figure 2. Main steps of cross-convolution approach

Note that in Theorem 2, δ is calculated without knowing or estimating the input coefficient b, which represents the product $K_{opt}n_0S$. This is one of the features of the proposed method because K_{opt} is usually unknown in practice.

The expression (7) includes the derivative of the output signal T_{out}. However, numerical differentiation of noisy signals is an ill-posed problem [19]. To overcome this ill-posedness, the following theorem is introduced.

Theorem 3 Let δ be unknown in (5), then it can be calculated as follows: $\forall t \in [0,\ t_f]$

$$\delta = \frac{\ln(\sqrt{\lambda})}{\gamma}, \tag{15}$$

where

$$\lambda = \frac{\int_0^t F^2(\theta)d\theta}{\int_0^t G^2(\theta)d\theta}, \tag{16}$$

such that

$$F(t) = \left[a_1 D^{-n+1} T_{out} - \psi_{-n,\,1}\{T_{out}\} + D^{-n}\left[a_2(T_{out} - T_{in}) + a_3(T_{mean} - T_a)\right]\right] * e^{-\gamma t}\ I(t), \tag{17}$$

$$G(t) = \Bigg[a_1\left[D^{-n+1}\left\{e^{-\gamma t}T_{out}\right\} - \psi_{-n,\,1}\{T_{out}\} + \gamma D^{-n}\{e^{-\gamma t}T_{out}\}\right]$$

$$+ D^{-n}\left\{a_2 e^{-\gamma t}(T_{out} - T_{in}) + a_3 e^{-\gamma t}(T_{mean} - T_a)\right\}\Bigg] * I(t), \tag{18}$$

$$\psi_{-n,\,1}\{T_{out}\} = \frac{1}{\Gamma(n)} t^{n-1}[T_{out}(t)]_{t=0}, \tag{19}$$

and $n \geq 1$.

Proof. The key point is to apply D^{-n} to (14). First, applying D^{-n} to the numerator of (14) and using (3) lead to:

$$D^{-n}\left[Y(t) * e^{-\gamma t}\ I(t)\right] = D^{-n}\left[Y(t)\right] * e^{-\gamma t}\ I(t). \tag{20}$$

However,

$$D^{-n}\left[Y(t)\right] = D^{-n}\left[a_1 D T_{out} + a_2(T_{out} - T_{in}) + a_3(T_{mean} - T_a)\right]$$

$$(\text{using Lemma 1}) = a_1 D^{-n+1} T_{out} - \psi_{-n,\,1}\{T_{out}\} + D^{-n}\left[a_2(T_{out} - T_{in}) + a_3(T_{mean} - T_a)\right], \tag{21}$$

where $\psi_{-n,\,1}\{T_{out}\}$ is given in (19). Second, applying D^{-n} to the denominator (14) and using (3) gives:

$$D^{-n}\left[e^{-\gamma t}Y(t) *\ I(t)\right] = D^{-n}\left[e^{-\gamma t}Y(t)\right] * I(t) \tag{22}$$

$$= \left[a_1 D^{-n}\{e^{-\gamma t} D T_{out}\} + D^{-n}\left\{a_2 e^{-\gamma t}(T_{out} - T_{in}) + a_3 e^{-\gamma t}(T_{mean} - T_a)\right\}\right] * I(t). \tag{23}$$

But by using the product rule for derivative, one can write

$$D\left\{e^{-\gamma t}T_{out}(t)\right\} = e^{-\gamma t} D T_{out} - \gamma T_{out} e^{-\gamma t}. \tag{24}$$

Hence, the first term in the R.H.S of (23) can be written as:

$$D^{-n}\left\{e^{-\gamma t}DT_{out}\right\} = D^{-n}\left\{D\left\{e^{-\gamma t}T_{out}\right\} + \gamma T_{out}e^{-\gamma t}\right\}$$

$$\text{(Using Lemma 1)} = D^{-n+1}\left\{e^{-\gamma t}T_{out}\right\} - \psi_{-n,\,1}\{e^{-\gamma t}T_{out}\} + \gamma D^{-n}[e^{-\gamma t}T_{out}], \tag{25}$$

where $\psi_{-n,\,1}\{e^{-\gamma t}T_{out}\} = \psi_{-n,\,1}\{T_{out}\}$ which is given in (19). Collecting the results in (21), (23), and (25) gives

$$e^{\gamma\delta} = \frac{F(t)}{G(t)}, \tag{26}$$

where F and G are those in (17) and (18), respectively. Finally, squaring, integrating, and then taking the natural logarithmic function to (26) completes the proof. □

5. Numerical simulation

This section presents a numerical demonstration of the efficiency and robustness of the proposed method. Firstly, the proposed model given in (5) is solved numerically by using the MATLAB package ode 45 where the model parameters and functions are set based on their real ranges as follows [20]: $C_{loop} = 3.287 \times 10^6$, $P_{cp} = 1.868 \times 10^6$, $S = 3,427$, $q = 0.0093$, $T_a = 20$, $T_{in} = 12$, $n_0 = 1$, $H_l = 500$, $K_{opt} = 0.6$, and $I(t) = 10t$. The step size and final time are set to $\Delta t = 0.01$ and $t_f = 300$, respectively.

5.1 *Adapted mathematical model*

Figure 3 depicts the outlet temperature when the time delay is not considered, $\delta = 0$, and when it is involved in the model. The figure demonstrates the effect of the time delay on the PTC. The impact of the time delay on the control problem of tuning the outlet temperature through the fluid flow rate will be presented and discussed in a forthcoming paper.

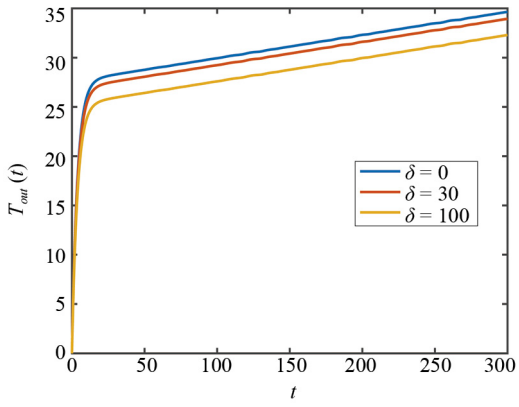

Figure 3. Outlet temperature with respect to different time delay values

5.2 *Delay estimation*

The efficiency of the estimation method given in Section 4 will be numerically demonstrated through different values for δ. For each value, noisy data is generated by adding a zero mean white Gaussian random noise to the measurement T_{out}, where the variance is chosen such that the Signal-to-Noise Ratio (SNR) has the values 40 dB and 25 dB.

The trapezoidal numerical integration method is used to numerically approximate integrals that appear in the proposed estimators. The tuning parameters γ and n are fixed to $\gamma = 10^{-4}$ and $n = 1$.

Figure 4 depicts the exact and noisy measurements when $\delta = 0.5$. Figure 5 (a) and Figure 5 (b) show the estimated time delay in noise-free case using Eq. (7) (Theorem 2) and Eq. (15) (Theorem 3), respectively, where $\delta = 0.5$. One can see that both estimators gave good results in the noise-free case.

In the noisy case, Figure 6 shows that the estimator in (7) failed to converge due to the differentiation of noisy data, see the paragraph before Theorem 3. Figure 7 shows that the estimator in (15) produced satisfactory results, even with a high level of noise, because it avoids differentiating noise measurements.

In Figure 8, the estimator in (15) has been examined in noisy cases for other time delay values: $\delta = 1,\ 1.5$, and 3.

The results presented here confirm the robustness and effectiveness of the filtered cross-convolution-based estimator for estimating delays in PTC, even when the measurements are corrupted by noise.

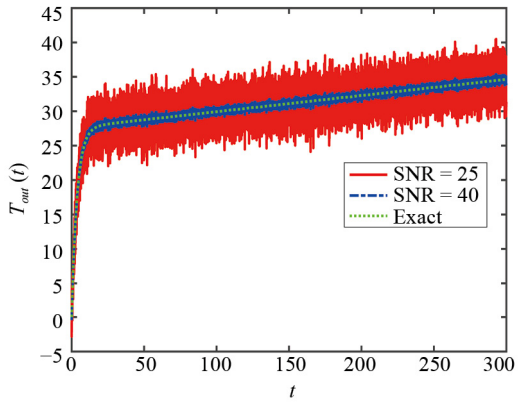

Figure 4. Exact and noisy outlet temperature (measurement), where $\delta = 0.5$

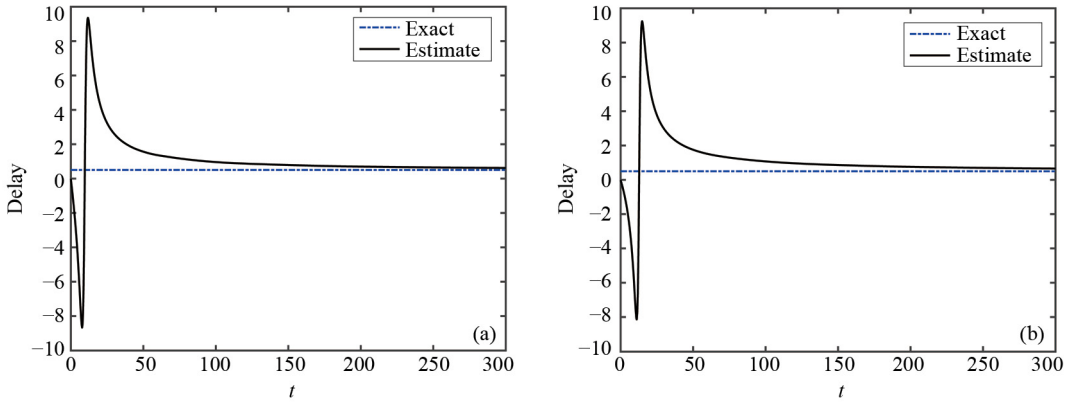

Figure 5. Estimated delay in noise-free case using: (a) Eq. (7) (Theorem 2), (b) Eq. (15) (Theorem 3), where $\delta = 0.5$

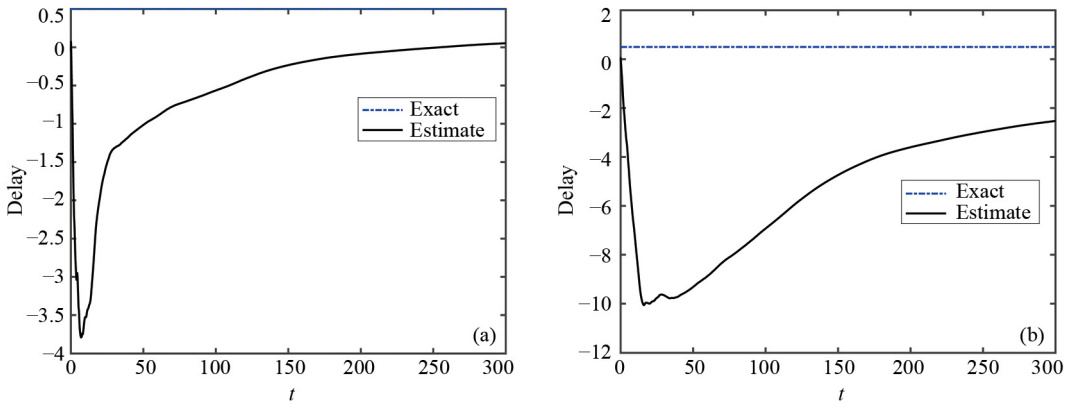

Figure 6. Estimated delay in noisy case using Eq. (7): (a) SNR = 40, (b) SNR = 25, where $\delta = 0.5$

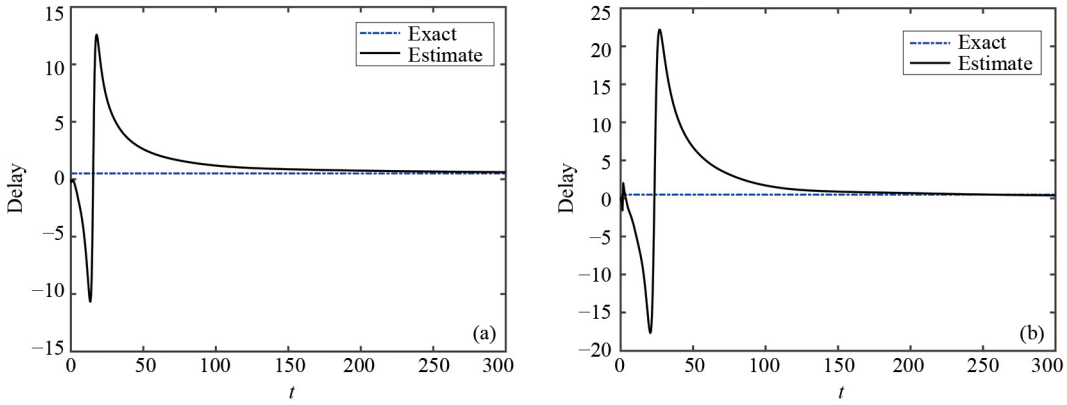

Figure 7. Estimated delay in noisy case using Eq. (15): (a) SNR = 40, (b) SNR = 25, where $\delta = 0.5$

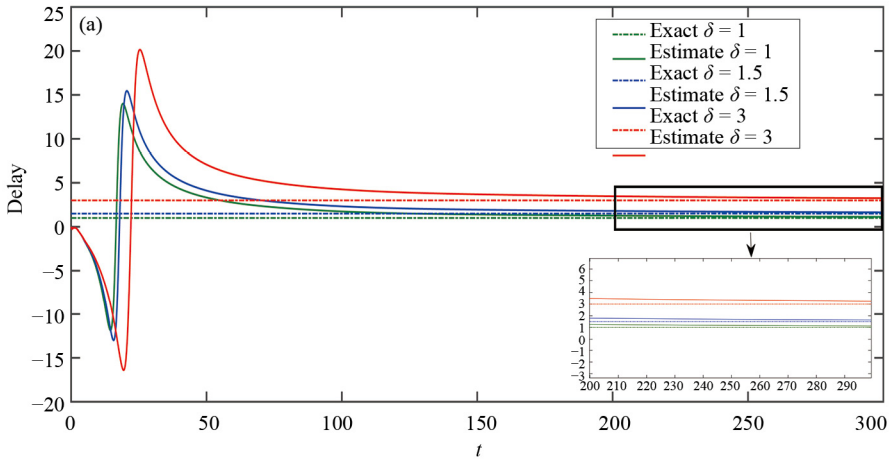

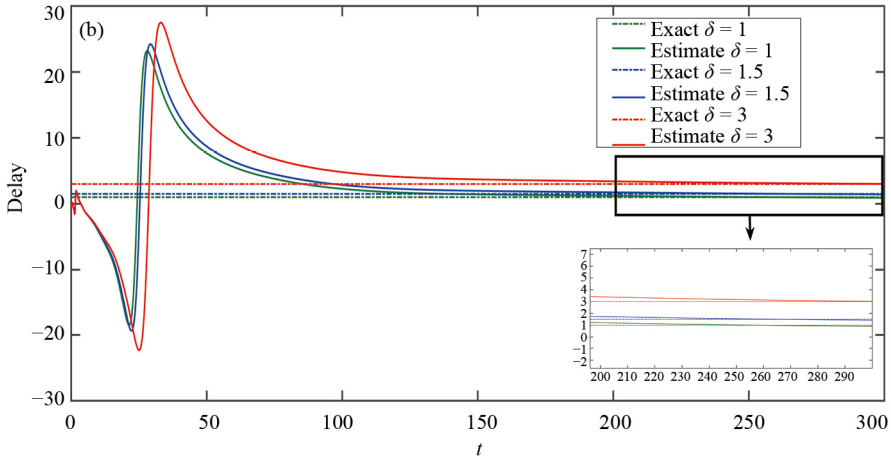

Figure 8. Estimated delay in noisy case using Eq. (15): (a) SNR = 40, (b) SNR = 25

5.3 *Comparing with modulating function-based method*

In this subsection, the delay estimation using the proposed cross-convolution method in (15) is compared with the modulating function-based method (MFBM) in [13]. In brief, the MFBM for estimating δ comprises the following steps:

(i) An initial guess for δ is chosen.

(ii) The MFBM is applied, and a nonlinear equation in δ is obtained.

(iii) The Gauss-Newton method is iterated to solve the nonlinear equation.

Figure 9 displays the comparable results of the two methods. One can observe that the MFBM converges faster; on the other hand, the cross-convolution approach is an initial guess-free method.

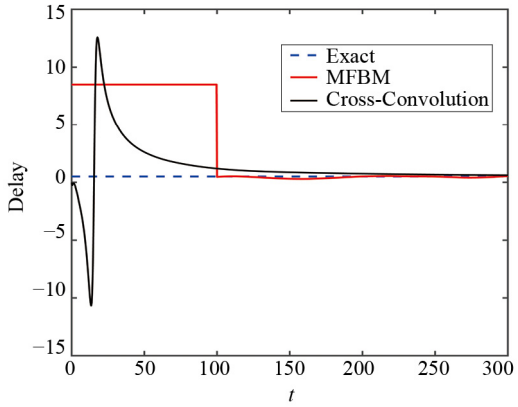

Figure 9. Exact delay $\delta = 0.5$ and estimated ones using the MFBM in [13] (red) and the filtered cross-convolution approach in (15) (black)

6. Conclusion

In this study, the mathematical model of the parabolic-trough solar collectors was extended by incorporating the possible time delay between the solar irradiance (input) and the outlet temperature (output). Since this time delay is uncertain or unknown in PTC, a method based on a cross-convolution approach was proposed to estimate it. Moreover, the efficiency of the proposed approach has been enhanced by integrating a filtering methodology. Numerical simulations

highlighted the significance of considering the time delay in the mathematical model as well as the robustness and effectiveness of the proposed estimation approach.

In future works, the extended mathematical model will be validated with real data. In addition, the effect of the time delay on model-based control techniques will be demonstrated.

Conflict of interest

The authors declare no competing financial interest.

References

[1] Voumik LC, Islam MA, Ray S, Yusop NYM, Ridzuan AR. CO_2 emissions from renewable and non-renewable electricity generation sources in the G7 countries: Static and dynamic panel assessment. *Energies*. 2023; 16(3): 1044.

[2] Sarbu I, Sebarchievici C. A comprehensive review of thermal energy storage. *Sustainability*. 2018; 10(1): 191.

[3] Camacho EF, Rubio FR, Berenguel M, Valenzuela L. A survey on control schemes for distributed solar collector fields. Part I: Modeling and basic control approaches. *Solar Energy*. 2007; 81(10): 1240-1251.

[4] Song Y, Zhang J, Li Y, Pan L, Liu Z. Temperature homogenization control of parabolic trough solar collector field. *IFAC-PapersOnLine*. 2023; 56(2): 5413-5418.

[5] Chanfreut P, Maestre JM, Krishnamoorthy D, Camacho EF. ALADIN-based distributed model predictive control with dynamic partitioning: An application to solar parabolic trough plants. In: *2023 62nd IEEE Conference on Decision and Control*. Singapore: IEEE; 2023. p.8376-8381.

[6] Mechhoud S, Laleg-Kirati TM. Adaptive energy-based bilinear control of first-order 1-D hyperbolic PDEs: Application to a one-loop parabolic solar collector trough. *Journal of the Franklin Institute*. 2018; 355(2): 827-848.

[7] Asiri S, Elmetennani S, Laleg-Kirati TM. Moving-horizon modulating functions-based algorithm for online source estimation in a first-order hyperbolic partial differential equation. *Journal of Solar Energy Engineering*. 2017; 139(6): 061007.

[8] Gallego AJ, Macias M, de Castilla F, Sánchez AJ, Camacho EF. Model predictive control of the mojave solar trough plants. *Control Engineering Practice*. 2022; 123(12): 105140.

[9] Zheng G, Polyakov A, Levant A. Delay estimation via sliding mode for nonlinear time-delay systems. *Automatica*. 2018; 89: 266-273. Available from: https: //doi.org/10.1016/j.automatica.2017.11.033.

[10] Barbot JP, Zheng G, Floquet T, Boutat D, Richard JP. Delay estimation algorithm for nonlinear time-delay systems with unknown inputs. *IFAC Proceedings Volumes*. 2012; 45(14): 237-241.

[11] Drakunov SV, Perruquetti W, Richard JP, Belkoura L. Delay identification in time-delay systems using variable structure observers. *Annual Reviews in Control*. 2006; 30(2): 143-158.

[12] Tuch J, Feuer A, Palmor ZJ. Time delay estimation in continuous linear time-invariant systems. *IEEE Transactions on Automatic Control*. 1994; 39(4): 823-827.

[13] Asiri S, Liu DY. Finite-time estimation for a class of systems with unknown time-delay using modulating functionsbased method. *Asian Journal of Control*. 2023; 25(2): 746-757.

[14] Belkoura L. Identifiability and algebraic identification of time delay systems. *IFAC Proceedings Volumes*. 2010; 43(2): 1-8.

[15] Asiri S, Liu DY. Cross-convolution approach for delay estimation in fractional-order time-delay systems. *Circuits, Systems, and Signal Processing*. 2024; 43(5): 2873-2890.

[16] Fliess M. Analyse non standard du bruit. *Comptes Rendus Mathematique*. 2006; 342(10): 797-802.

[17] Podlubny I. *Fractional Differential Equations*. New York: Academic press; 1999.

[18] Wei YQ, Liu DY, Boutat D, Liu HR, Wu ZH. Modulating functions based model-free fractional order differentiators using a sliding integration window. *Automatica*. 2021; 130: 109679.

[19] Liu DY, Gibaru O, Perruquetti W, Laleg-Kirati TM. Fractional order differentiation by integration and error analysis in noisy environment. *IEEE Transactions on Automatic Control*. 2015; 60(11): 2945-2960.

[20] Sánchez A, Gallego A, Escano J, Camacho E. Thermal balance of large scale parabolic trough plants: A case study. *Solar Energy*. 2019; 190: 69-81. Available from: https: //doi.org/10.1016/j.solener.2019.08.001.